Seventh International Conference on CFD in the Minerals and Process Industries
CSIRO, Melbourne, Australia
9-11 December 2009

CFD DESIGN OF A GENERIC CONTROLLER FOR VORTEX-INDUCED RESONANCE

Andrew A. ANTIOHOS, S. Eren SEMERCIGIl and Özden F. TURAN

School of Engineering and Science, Victoria University, Melbourne, Victoria 8001, AUSTRALIA

ABSTRACT

A simple control technique is proposed in this paper to avoid the organisation of the resonance vibrations of a lightly damped structure. The control principle is based on interfering with the establishment of the naturally organised process of structural resonance. To implement the control, fluctuations are introduced in the natural frequency of the structure. Hence, the proposed technique is a semi-active parameter control. Numerical case studies are presented, using an elastically suspended circular cylinder exposed to vortex-induced resonance, to search for the most effective fluctuation.

NOMENCLATURE

C_L	lift coefficient
c	damping constant
D	cylinder diameter
F_L	lift force
f_n	structural natural frequency
f_{vo}	vortex shedding frequency
k	spring constant
m	cylinder mass per unit length
Re	Reynolds number
St	Strouhal number
t	time
T_c	control period
T_n	undamped natural period of the cylinder
U_o	free stream velocity
y	vertical position of the cylinder
υ	kinematic viscosity
ζ	critical viscous damping ratio

INTRODUCTION

As flow passes over a resonant structure, such as a marine riser used for off-shore drilling, the vortices that are shed as a result of obstructing the flow, may induce significantly large levels of vibration. When the vortex shedding frequency approaches the natural frequency of the structure, structural oscillations grow and start establishing a strong interaction with the shedding mechanism in the flow. Resulting structural resonance is detrimental for safety. Therefore, it is important to develop concepts for controlling structural resonance. Some recent work to reduce the effects of vortex induced vibration includes that of Bearman and Brankovic (2004), in which strakes and bumps have been used on circular cylinders. They concluded that passive suppression devices prevent the regular vortex shedding pattern. However, a build up of vibration still occurs for a flexible cylinder if the reduced velocity is in the range of the critical natural frequency. Kumar et al. (2008) also suggest the addition of passive control devices for marine structures, such as streamlining the geometry and applying add-on features. Although these devices provide effective control, they can affect the aerodynamic performance, cost and simplicity of the structure.

The objective of this paper is to present a progress report of numerical predictions for a proposed control technique, designed to prevent the formation of organised vortex-induced resonance. The proposed technique is a semi-active parameter control, which corresponds to a mechanical system with a variable effective length, resulting in variable natural frequency through variable structural stiffness.

MODEL DESCRIPTION

The model of the circular cylinder for the two-dimensional flow simulations is shown in Figure 1. The cylinder is assigned a mass (m), stiffness (k) and a viscous damping coefficient (c). The model represents the dynamics of a simple structure at one vibration mode, most likely the fundamental one. This single degree of freedom (SDOF) system is allowed to oscillate in cross-flow (y-direction in Figure 1), perpendicular to the flow which travels from left to right. The model is fixed in the flow direction.

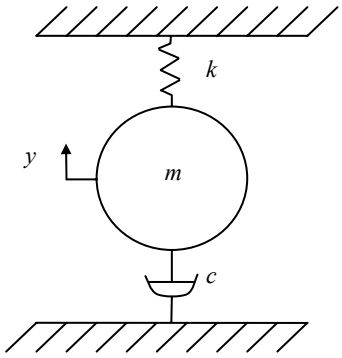

Figure 1: Schematic representation of the elastically mounted circular cylinder in cross-flow.

The spring constant and mass were chosen such that the structural resonance corresponds to a Reynolds number, $Re = U_o D/\upsilon$, of 1000, where U_o is the free stream velocity, D is the cylinder diameter and υ is the kinematic viscosity. This assertion of structural resonance is possible due to the Strouhal number, $St = f_{vo} D/U_o$, having the value of 0.2 for a wide range of Re for a circular cross-section (Blevins 1990). In the definition of St, f_{vo} is the vortex shedding frequency. The damping constant, c, was chosen to represent two different critical viscous damping ratios, ζ of 1% and 5%.

The software package, *FLUENT*, has been used to perform the flow simulations. As flow travels over the elastically mounted circular cylinder, unsteady pressure fluctuations act on its surface as a result of vortex shedding, causing it to oscillate in the y-direction. To obtain the flow field predictions with the moving boundary of the elastically mounted cylinder, a user defined function (UDF) was written in C language. The objective of this UDF is to communicate with *FLUENT* to determine the motion of the SDOF system using the equation of motion:

$$F_L = m\ddot{y} + c\dot{y} + k y \qquad (1)$$

Here, F_L is the sum of the pressure and viscous forces on the cylinder boundary in the y-direction. Over-dots represent time derivatives. The UDF calculates y in response to the fluid loading, F_L at every time step. This is performed by rearranging (1) to give the instantaneous change in velocity as:

$$d\dot{y} = \frac{\left(F_L - c\dot{y} - k y\right)}{m} dt \qquad (2)$$

The resulting velocity calculated in (2) is interpreted by *FLUENT* to update the vertical position of the cylinder boundary. *FLUENT* re-meshes the computational domain in response to the new position of the boundary at each time step.

The full computational domain for the numerical simulations is presented in Figure 2(a). The domain is similar to that used by Tutar and Holdo (2000), as it extends from the center of the cylinder a distance of 7*D* both upstream and along the y-direction and a distance of 15*D* downstream. This ensured sufficient space for the downstream wake development, as well as minimising blockage effects due to boundaries in the y-direction.

The velocity inlet boundary condition was set for *Re* ranging from 800 to 1100. Pressure inlet boundary conditions were applied to the top and bottom boundaries and a pressure outlet boundary condition was applied to the downstream boundary, as shown in Figure 2(a).

The mesh used is an unstructured triangular mesh of 36338 cells. This mesh allowed appropriate input variables to be applied in *FLUENT* for a fixed-grid configuration during simulations, as the mesh moved with the cylinder motion. This approach is similar to that implemented by Blackburn and Karniadakis (1993). A size function was used starting from the cylinder wall, in order to ensure a fine enough mesh to sufficiently resolve the boundary layer, while minimising the effect on computational time. This is shown in Figure 2(b). In order to capture the vortex shedding accurately, the time step, *dt*, was set at 0.001 s, to ensure at least 600 time steps are used per shedding cycle.

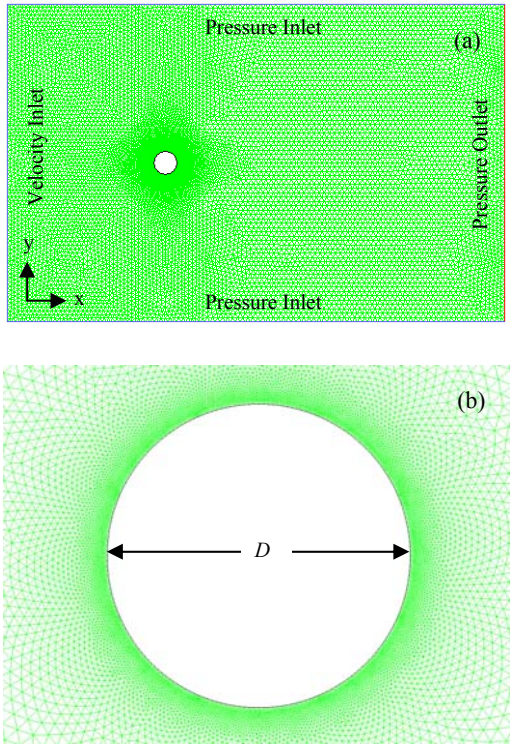

Figure 2: Showing (a) Full computational domain with imposed boundary conditions and (b) Enlarged view with concentrated computational nodes.

NUMERICAL OBSERVATIONS

Uncontrolled Vortex-Induced Resonance

In order to determine the free stream velocity at which vortex induced resonance occurred, simulations were conducted for *Re* of 800, 850, 900, 1000 and 1100. The reason for needing to search for resonance is due to the structural resonance being designed for a *Re* of 1000 in vacuum. The added mass effect of the fluid mass around the cylinder could change this *Re*. Hence, the *Re* range can also be interpreted to correspond to the frequency ratios of excitation, f_{vo}/f_n, of 0.8, 0.85, 0.9, 1 and 1.1, where f_n is the structural natural frequency in vacuum.

In Figure 3, the displacement history for the uncontrolled vibration for the range of *Re* at 1% critical damping is shown. Non-dimensional time, t/T_n, is shown along the horizontal axis, where T_n is the undamped natural period of the structure. Vertical axes indicate both the lift coefficient, C_L, and the non-dimensional displacement magnitude, y/*D*. Simulations are performed for 25 natural periods to maintain reasonable computational times.

Oscillations of the elastically mounted circular cylinder generally occur simultaneously at the vortex shedding frequency and structural frequency. Therefore, the existence of two close frequencies creates a beat envelope of different periods, depending on the value of the frequency ratio, f_{vo}/f_n. In Figures 3(a) and 3(c), the beat period is approximately $15T_n$, in 3(d) it is $7T_n$ and finally in 3(e) it is $4T_n$.

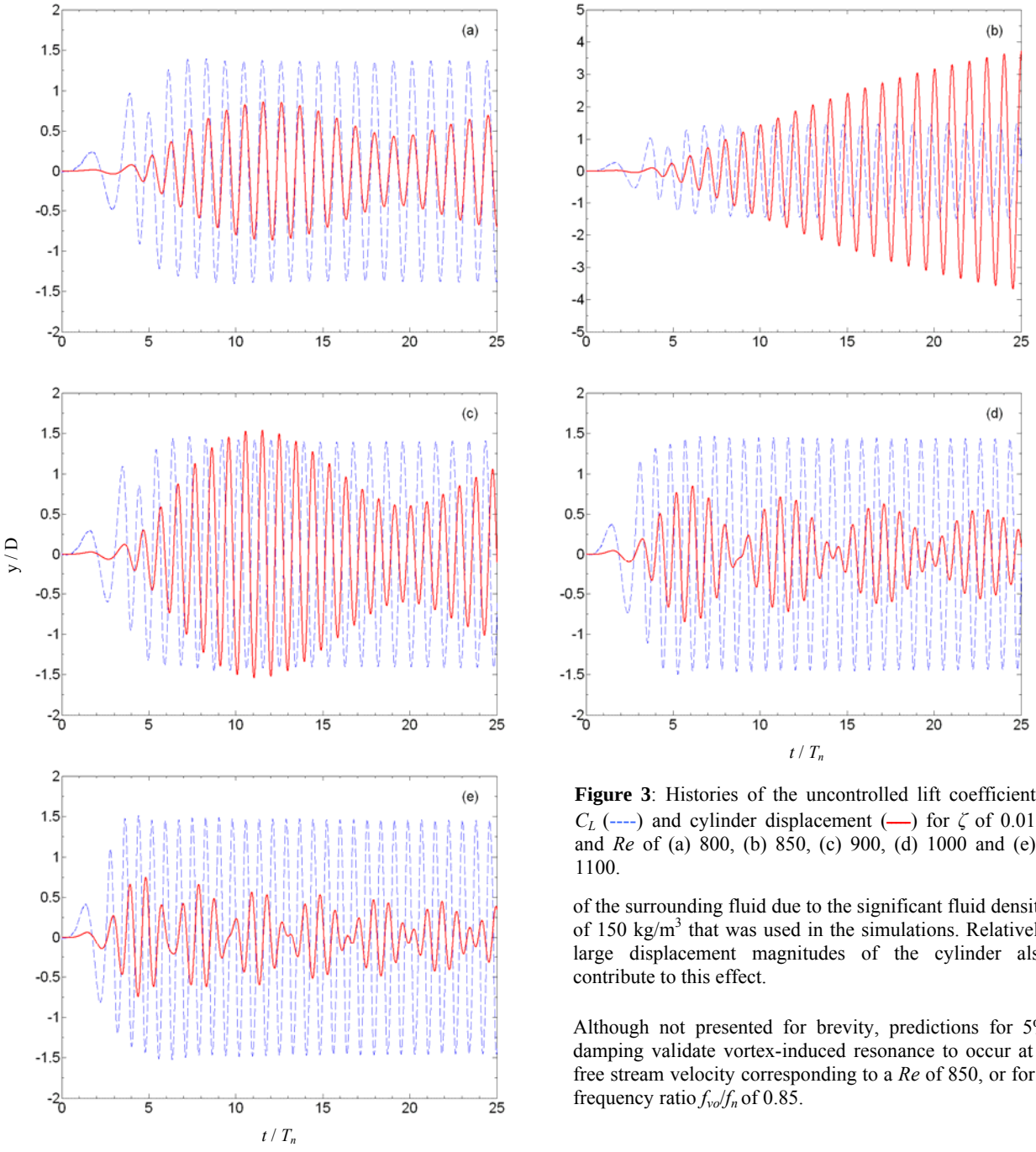

Figure 3: Histories of the uncontrolled lift coefficient C_L (----) and cylinder displacement (—) for ζ of 0.01 and Re of (a) 800, (b) 850, (c) 900, (d) 1000 and (e) 1100.

A long beat period indicates two spectral components of comparable magnitudes at close frequencies, whereas a short beat period is the result of these frequencies moving away from each other.

In Figure 3(b) no beat is observed, as there is close agreement between the vortex shedding and structural frequencies, therefore, suggesting the presence of structural resonance. This suggestion is supported by the existence of the growing envelope of the displacement history and the consistent quarter cycle phase lead between the lift coefficient and cylinder displacement histories (Dimarogonas and Haddad 1992). Hence, vortex-induced resonance is observed at a frequency ratio f_{vo}/f_n of 0.85, not at 1. A shift in the structural resonance frequency of approximately 15% can be attributed to the added mass of the surrounding fluid due to the significant fluid density of 150 kg/m^3 that was used in the simulations. Relatively large displacement magnitudes of the cylinder also contribute to this effect.

Although not presented for brevity, predictions for 5% damping validate vortex-induced resonance to occur at a free stream velocity corresponding to a Re of 850, or for a frequency ratio f_{vo}/f_n of 0.85.

Proposed Control

The implementation of the control involves fluctuating the structural stiffness, $k(t)$, in a square wave fashion, at a pre-determined control period, T_c. The choice for the square wave is purely for simplicity, which may well be altered during the later development stages. It is believed this application should provide an effective suppression technique, as it interferes with the organisation of vortex induced resonance. Simply changing the structural resonance frequency instead of fluctuating it, will only allow the problem to occur at another free-stream velocity and Re.

The proposed control is a semi-active parameter control technique. It contains a significant simplification that the actuation period is decided as part of design, not as part of flow or oscillation conditions. Therefore, no sensing or

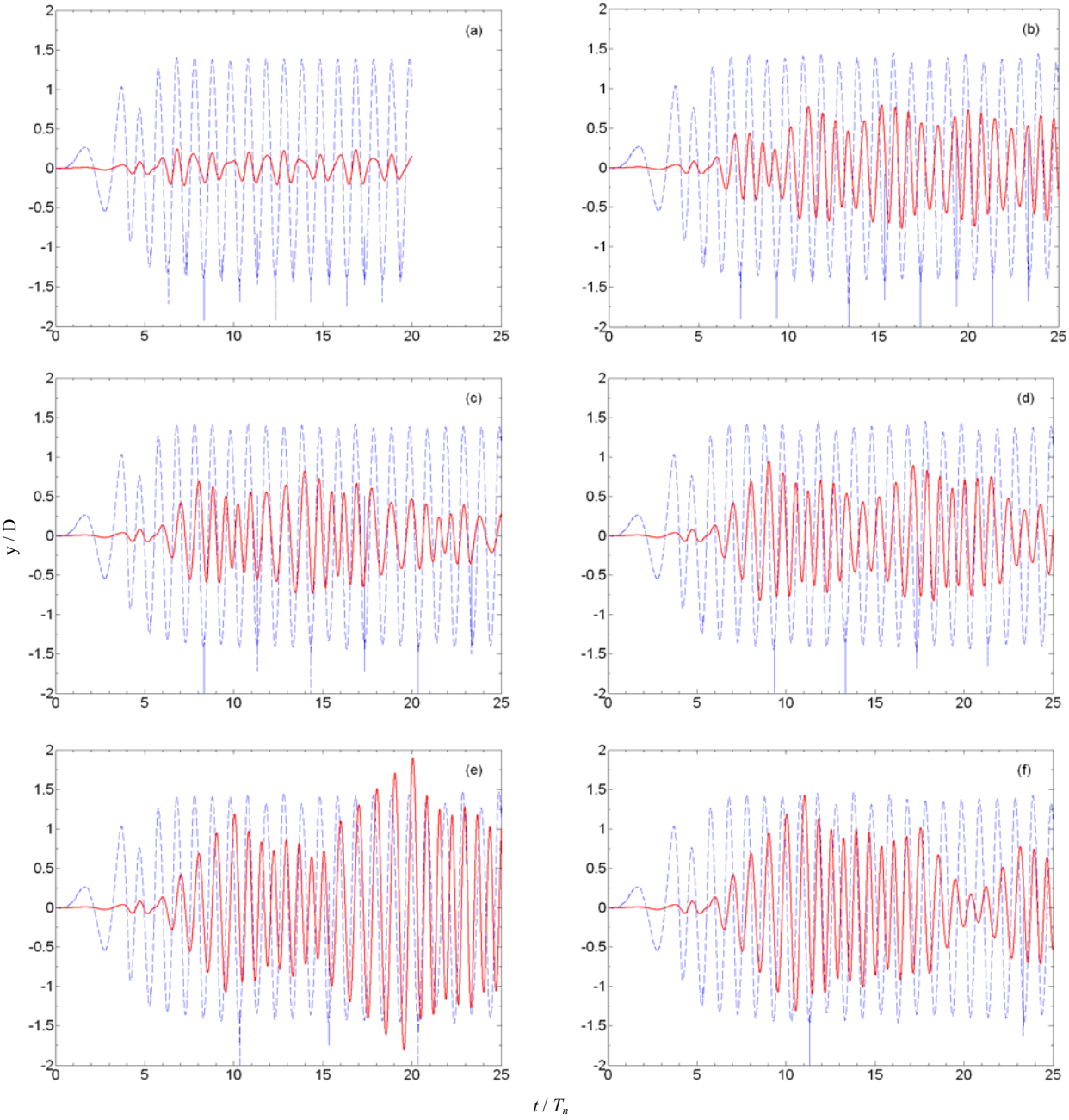

Figure 4: Histories of the controlled lift coefficient C_L (----) and cylinder displacement (—) for ζ of 0.01, *Re* of 850 and for actuation periods, T_c of (a) T_n, (b) $2T_n$, (c) $3T_n$, (d) $4T_n$, (e) $5T_n$ and (f) $6T_n$.

computing would be required for actuation of the control. For this reason, it is important to determine the most practical magnitude and period of actuation as key design variables.

Simulations were performed with variations in the spring constant from k, as the starting point, up to a magnitude of αk. The smallest α to provide a significant enough suppression of vortex induced resonance was determined to be 2.

For practical applications, it is also desirable that the actuation frequency of the stiffness fluctuations is small, while still maintaining effectiveness in control. Different control periods, T_c, were analysed between T_n to $6T_n$.

The displacement history of the controlled response for control intervals T_c of T_n, $2T_n$, $3T_n$, $4T_n$, $5T_n$ and $6T_n$ at the frequency ratio, f_{vo}/f_n of 0.85 is shown in Figure 4. The axes are the same as in Figure 3. The sharp peaks shown in the lower half of the C_L history indicate the actuation of the control. An initial delay of $5T_n$ was applied before the first actuation, in order to let the initial transient conditions of the numerical solution to settle.

It can be seen in Figure 4 that applying a fluctuation to the stiffness significantly prevents the organised resonance structure, as the amplitude ratio, y/D is significantly smaller than that of the uncontrolled case in Figure 3(b). The most effective case is presented in Figure 4(a) with the control applied at every natural period, T_n, with the

largest y/D of 0.25. As the displacement and C_L histories shown in Figure 4(a) are now in-phase, the structural resonance is prevented successfully. However, an actuation period equal to the natural period of the structure may be too rapid for a mechanical system to apply reliably.

In Figures 4(b), 4(c) and 4(d), corresponding to T_c of $2T_n$, $3T_n$ and $4T_n$, respectively, the maximum magnitudes of oscillation for the elastically mounted circular cylinder are comparable. The displacements do not increase and the motion is non-resonant. Therefore, a control period as long as $4T_n$ can still be an effective solution.

The reduced amplitudes, y/y_o, for different control periods are shown in Figure 5. Here, y_o is the uncontrolled cylinder displacement at f_{vo}/f_n of 0.85, obtained at t/T_n of 25. As the maximum uncontrolled cylinder displacement does not occur at 25 natural periods, these reduced amplitudes should represent conservative estimates of effectiveness. The envelope indicates the variation between the maximum and minimum amplitudes observed for each case after 10 natural periods. The vertical axis represents the effectiveness of control, as values of 1 and 0 represent an uncontrolled cylinder and the perfectly controlled cylinder, respectively.

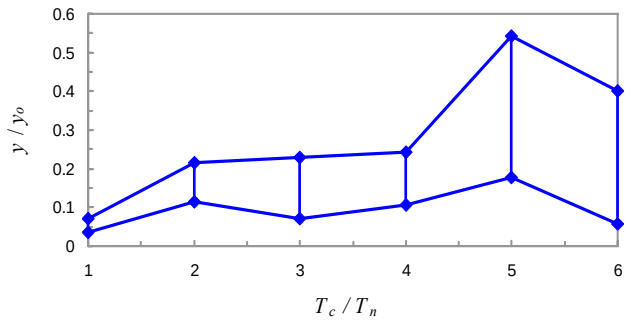

Figure 5: Variation of the amplitude ratio, y/y_o with control period, T_c.

As expected, effectiveness in control decreases gradually for an increasing control period. In addition, the envelope of controlled displacements fluctuates by wider margins for increasing control periods, indicating a less consistent response.

It is noted in Figures 3 and 4 that the C_L histories display very similar patterns for all simulations. The maximum amplitude of lift is approximately 1.5 for both the uncontrolled and controlled cases. This suggests that there may be significant similarities in the vortex wake pattern for all these cases.

Contours of vorticity magnitude for the controlled cylinder at f_{vo}/f_n of 0.85 and T_c of T_n are presented in Figure 6, obtained near t/T_n of 20. This corresponds to incidents when a vortex is about to shed from the top of the cylinder. The colour scale represents the magnitude of vorticity. The largest magnitude of vorticity is located along the surface of the cylinder, near the stagnation point. The vortex pattern shown in Figure 6 remains constant for all uncontrolled and controlled cases. This is also similar

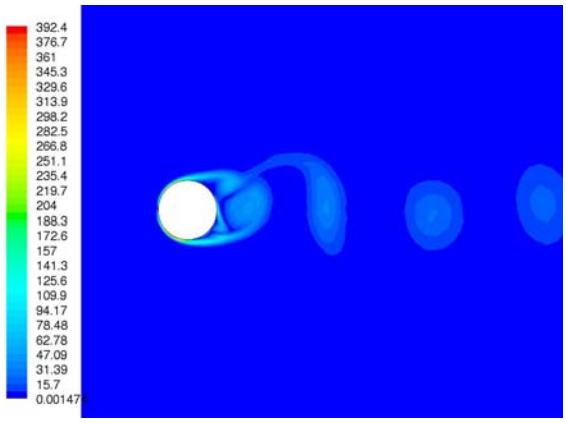

Figure 6: Contours of vorticity magnitude for ζ of 0.01 and Re of 850 near t/T_n of 20 for T_c of T_n.

to that of a stationary circular cylinder, not shown for brevity. This suggests that the shedding of vortices occurs for the same cylinder position during oscillations in the vertical direction. Analysis of the simulations determined that shedding occurs when the cylinder reaches zero displacement and the vortices are developed as the cylinder reaches its peak vertical displacement. Therefore, this indicates that two vortices are present during each period of motion.

The vortex pattern shown in Figure 6 corresponds to the 2S vortex wake mode defined as two single vortices per cycle of motion by Williamson and Govardhan (2004). They show experimentally that the 2S mode occurs for amplitude ratios y/D between 0.2 and 0.4. Numerical observations for the controlled cylinder are in close agreement, as the maximum amplitude ratios shown in Figure 4 are between 0.25 and 0.85 for T_c of T_n to $4T_n$, respectively. However, for the uncontrolled case at f_{vo}/f_n of 0.85 the cylinder displacement is significantly larger than the suggested range of y/D, yet the same 2S vortex wake pattern is predicted numerically. This is currently under investigation.

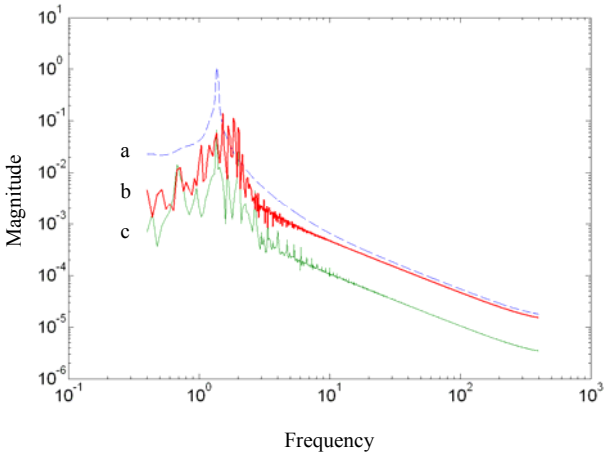

Figure 7: Frequency distribution for the uncontrolled cylinder (a, ----) and controlled cylinder at T_c of $4T_n$ (b, —) and T_n (c, —).

The frequency distributions of the predicted cylinder displacement at f_{vo}/f_n of 0.85 for the uncontrolled and controlled cases at T_c of T_n and $4T_n$ are presented in Figure 7. The uncontrolled cylinder predominantly oscillates at a peak frequency of 1.36 Hz, similar to the vortex shedding frequency of 1.33 Hz for *St* of 0.2. For the controlled cases, a dominant frequency is not as clear to identify as many spectral components co-exist with comparable magnitudes. This behaviour is a result of successfully preventing an organised structural resonance with the implementation of stiffness variations. As discussed earlier in relation to Figure 4, a control period of T_n results in significantly smaller displacements than those for $4T_n$.

PRACTICAL IMPLEMENTATION

The proposed control could benefit a cantilevered structure, or a structure with a significant free span between supports, similar to a marine riser that is exposed to vortex induced resonance. A mechanical system could implement the control, possibly by applying and removing a clamp to change the effective free length, therefore, varying the effective stiffness. The location and the timing of the clamp are determined as part of the controller design. No sensing or computing would be required for actuation.

CONCLUSION

A brief summary of a numerical case study is presented in this paper to avoid vortex induced resonance. An elastically mounted circular cylinder exposed to cross-flow is modelled using *FLUENT* to investigate both uncontrolled and controlled vibration conditions.

Due to the added mass of the fluid surrounding the structure, a search for resonance was conducted. Numerical observations determined resonance to occur near a free-stream velocity corresponding to a *Re* of 850 for the simulation parameters.

A semi-active parameter control is then implemented practically by varying the effective stiffness. It has been observed that a square wave fluctuation between the original and doubled structural stiffness, and an actuation period equal to the structural natural period provides the best control for resonance. The proposed application effectively prevents the organised resonance structure.

Numerical observations show similar vortex wake patterns for all studied cases with a 2S vortex wake mode. This mode is in good agreement with published experimental results for the controlled cases. However, the uncontrolled case at resonance also contains the 2S mode with a significantly larger amplitude ratio than what has been reported in literature. It is considered at this point that this anomaly may be due to not reaching a steady state pattern of oscillations at the time of the comparison.

The observations presented in this paper provide a positive outcome for the continuation of the investigation to consider the aerodynamic performance, cost and practicality.

REFERENCES

BEARMAN, P. and BRANKOVIC, M., (2004), "Experimental Studies of Passive Control of Vortex-Induced Vibration", *European Journal of Mechanics B/Fluids*, 23, 9-15.

BLACKBURN, H.M. and KARNIADAKIS, G.E., (1993), "Two- and Three-Dimensional Simulations of Vortex-Induced Vibration of a Circular Cylinder", In '*3rd International Offshore and Polar Engineering Conference*', Singapore, 715-720.

BLEVINS, R.D., (1990), "Vortex-Induced Vibration", In '*Flow-Induced Vibration*', 47-49. (Van Nostrand Reinhold: New York).

DIMAROGONAS, A.D. and Haddad, S., (1992), "Forced Harmonic Vibration", In '*Vibration for Engineers*', 126-128. (Prentice-Hall, Inc.: New Jersey).

KUMAR, R.A., Sohn, C-H. and Gowda, B.H.L., (2008), "Passive Control of Vortex-Induced Vibrations: An Overview", *Recent Patents on Mechanical Engineering*, 1, 1-11.

TUTAR, M. and Holdo, A.E., (2000), "Large Eddy Simulation of a Smooth Circular Cylinder Oscillating Normal to a Uniform Flow", *Journal of Fluids Engineering*, 122, 694-702.

WILLIAMSON, C.H.K. and GOVARDHAN, R., (2004), "Vortex-Induced Vibrations", *Annual Review of Fluid Mechanics*, 36, 413-455.

